Weathering damage on Pharaonic sandstone monuments in Luxor - Egypt

Bernd Fitzner*, Kurt Heinrichs, Dennis La Bouchardiere

Geological Institute, Aachen University, Working group „Natural stones and weathering“, Wuellnerstrasse 2, D-52062 Aachen, Germany

Abstract

The Pharaonic stone monuments in Upper Egypt represent cultural heritage of outstanding universal value. All monuments have suffered weathering damage. In the year 2000 an Egyptian-German research co-operation was started aiming at the systematic investigation of stone weathering on the historical monuments in Upper Egypt as a contribution to monument preservation. Pilot studies were carried out on the Karnak Temple and on the Luxor Temple, composed of sandstones originating from the Gebel el-Silsila region. First results on the petrographical properties of these sandstones and their state of weathering damage on the Pharaonic temples in Luxor are presented.

Keywords: Pharaonic monuments; Karnak Temple; Gebel el-Silsila sandstones; Weathering forms; Monument mapping; Damage index

1. Introduction

Upper Egypt is well-known for its famous Pharaonic stone monuments. They give testimony of the unique creative work of humankind in ancient times. The monuments are significant for the cultural identity of Egypt and they are very important for the economic situation of the country. Sandstones, limestones and granites represent the characteristic stone types used for the construction of the Pharaonic monuments in Upper Egypt. Since their construction, the monuments have suffered stone weathering. The preservation of the monuments has become an ever-increasing challenge.

The improvement of knowledge about the natural stones used and about the factors, processes and characteristics of stone weathering as a basis for sustainable monument preservation is the aim of an Egyptian-German research co-operation that was initiated in the year 2000. In co-operation with the Egyptian Supreme Council of Antiquities and the Institute of Restoration / Luxor, initial studies were carried out on sandstone monuments, in particular on Luxor Temple and especially on Karnak Temple in Luxor (Fig. 1-4), which represent two of the most important sandstone monuments of ancient Thebes that was inscribed on the UNESCO World Heritage List as “a striking testimony to Egyptian civilisation at its height”.

Sandstones from the Gebel el-Silsila area in south-western Egypt – as one group of the formerly so-called „Nubian sandstone“ – were used for the construction of Karnak Temple and Luxor Temple and these sandstones are still used in the course of stone replacement. Sandstone samples for petrographical studies were taken from historical quarries. Initial in situ studies on the weathering damage on the monuments comprised survey, classification and registration of weathering forms. The detailed registration of the weathering forms was made by means of monument mapping. The registration and evaluation of weathering forms were focussed on Karnak Temple, taking into account the remarkable complexity of construction phases, architectonical composition, lithotypes, exposure characteristics and previous preservation measures.

*Corresponding author. Tel.: +49-241-8095727, Fax: +49-241-8092346.
E-mail address: fitzner@geol.rwth-aachen.de (B. Fitzner).

Building and Environment (2003), Vol. 38, Issues 9-10, Building stone decay: observations, experiments and modeling, 1089-1103, Elsevier Ltd. 1089-1103. doi: 10.1016/S0360-1323(03)00086-6

Initial results on the petrographical properties of the Gebel el-Silsila sandstones and on the range of their weathering forms – considering types and intensities – are presented. Furthermore, the rating of weathering damage on the sandstone monuments by means of damage categories and damage indices is explained and demonstrated by means of examples.

Fig. 1. Karnak Temple. Avenue of the Sphinxes and 1st Pylon.

Fig. 2. Karnak Temple. Sacred lake, Column hall and 1st Pylon.

Fig. 3. Luxor Temple. Avenue of the Sphinxes and Great Pylon.

Fig. 4. Luxor Temple. Great Pylon and Court of Ramesses II.

2. Petrographical properties of Gebel el-Silsila sandstones

Sandstones from the Gebel el-Silsila region were used for the construction of most of the sandstone monuments in Upper Egypt as well as in the course of past and current restoration works. The Gebel el-Silsila area is located in south-western Egypt, about 160 km south of Luxor and 50 km north of Aswan. The sandstone quarries extend over the west and east banks of the Nile (Fig. 5 and 6).

The Gebel el-Silsila sandstones – representing one group of the formerly so-called “Nubian Sandstone” – are stratigraphically attributed to the Qoseir-Formation of the Lower Campanian / Upper Cretaceous (HERMINA, KLITZSCH & LIST [1], TAWADROS [2]).

Regarding the petrographical properties of the Gebel el-Silsila sandstones, studies by other authors have mainly concerned the mineralogical and geochemical composition of the sandstones (e.g. ABD EL HADY [3, 4], MARTINET [5], KLEMM & KLEMM [6]). These studies already revealed considerable variation in the sandstones.

Within the framework of this research project, a detailed differentiation and classification of the Gebel el-Silsila sandstones is aimed at, and which is essential for:

- information on the provenance of the stone materials used on the monuments,
- quantification, evaluation and interpretation of the weathering behaviour of the different sandstone varieties,
- rating of stone quality and stone durability,
- damage prognosis,
- development of weathering models,

- derivation of appropriate preservation measures.

This will necessitate a precise survey of the many historical quarries and systematic sampling. During the first field campaign, several sandstones have already been sampled from different historical quarries on the east bank and the west bank of the Nile in the Gebel el-Silsila region for pilot petrographical and petrophysical studies. These studies comprised:

- macroscopical description,
- identification of mineral components by means of X-ray diffraction analysis (XDA),
- determination of the mineral composition, matrix-grain-ratio, grain size distribution, mean grain size, sorting as well as characterization and quantification of grain contacts by means of transmitted light microscopy with image analysis,
- quantification of porosity characteristics such as densities, total porosity, median pore radius, median radius of pore entries and pore surface by combined application of mercury porosimetry, nitrogen adsorption method and transmitted light microscopy with image analysis,
- first studies on petrophysical properties by means of ultrasonic measurements and drilling resistance measurements.

The sandstone classification was made according to PETTIJOHN et al. [7], the grain size classification according to WENTWORTH (in PETTIJOHN et al. [7]) and the mean grain size and sorting were determined according to TRASK (in TUCKER [8]). Ultrasonic measurements were made parallel and perpendicular to bedding. The ratio between the ultrasonic velocity parallel to bedding and the ultrasonic velocity perpendicular to bedding was defined as the anisotropy index.

Initial results on petrographical and petrophysical properties are presented for four Gebel el-Silsila sandstones (Fig. 7). The results are summarized in the following sections.

Fig. 5. Gebel el-Silsila/west-bank, Ptolomaic quarry.

Fig. 6. Gebel el-Silsila/east-bank, Great Ptolomaic quarry.

2.1. Sandstone 1

This light brown, spotted sandstone was quarried for stone replacement works at the Karnak Temple. It is composed of quartz (main component), rock fragments, clay minerals (kaolinite, clinochlore), opaque matter, feldspar (microcline, albite), mica (muscovite) and heavy minerals. Compared with the other sandstones, it shows the highest contents of rock fragments, feldspar and mica. The content of matrix minerals and, thus, the matrix-grain-ratio is rather low. The sandstone can be classified as a sublitharenite.

The sandstone is fine-grained. The proportion of grains in the class of coarse silt (0.031 – 0.063 mm) is low to medium, medium to high in the class of very fine sand (0.063 – 0.125 mm), high (main peak) in the class of fine sand (0.125 – 0.25 mm), medium in the class of medium sand (0.25 – 0.5 mm) and very low in the class of coarse sand (0.50 – 1.00 mm). Compared with

the other sandstones, it shows the highest proportions of grains in the classes of medium sand and coarse sand. The sorting of the sandstone is moderate. Point contacts of the grains are dominant. Compared with the other sandstones, it shows the lowest number of grain contacts.

The total porosity of the sandstone is high. Interparticle porosity is characteristic. Large capillary pores with rather large pore entries are dominant. The proportion of micropores (radius < 0.1 µm) is low. Compared with the other sandstones, it shows the largest median pore radius and a medium pore surface. The ratio between the median radius of pore entries and the median pore radius is the lowest for the studied sandstones.

The sandstone is characterized by rather low ultrasonic velocities and low drilling resistance (hardness). The anisotropy index reveals moderate anisotropical properties of the sandstone.

2.2. Sandstone 2

This white, spotted sandstone was also quarried for stone replacement works at the Karnak Temple. It is mainly composed of quartz (main component), rock fragments, clay minerals (kaolinite, clinochlore), opaque matter, feldspar (albite), mica (muscovite) and heavy minerals. Additionally, in this sandstone small contents of calcite and gypsum were found. Compared with the other sandstones, it shows the lowest content of clay minerals. The content of matrix minerals and the matrix-grain-ratio are rather low. The sandstone can be classified as sublitharenite.

The sandstone is fine-grained. The proportions of grains in the class of coarse silt is low to medium, medium to high in the class of very fine sand, very high (main peak) in the class of fine sand, low to medium in the class of medium sand and very low in the class of coarse sand. Compared with the other sandstones, it shows the highest proportion of grains in the class of fine sand. The sorting of the sandstone is good. Point contacts and long contacts of the grains are dominating. Comparing the four sandstones, it shows a medium number of grain contacts.

The total porosity of the sandstone is very high. Interparticle porosity is characteristic. Large capillary pores with rather large pore entries are dominant. The proportion of micropores is low. Compared with the other sandstones, it shows a small pore surface.

The sandstone is characterized by low to medium ultrasonic velocities and low drilling resistance. The anisotropy index reveals moderate anisotropical properties of the sandstone.

		Sandstone 1	Sandstone 2	Sandstone 3	Sandstone 4
Lithotype	Provenance	Gebel el-Silsila, east-bank, stone replacement material at Karnak Temple	Gebel el-Silsila, east-bank, stone replacement material at Karnak Temple	Gebel el-Silsila, west-bank, Great North quarry	Gebel el-Silsila, east-bank, Great Ptolomaic quarry
	Description	Light brown, spotted, fine-grained sandstone	White, spotted, fine-grained sandstone	Yellow-brown, very fine- to fine grained sandstone	White, fine-grained sandstone
	Stratigraphy	Qoseir Formation – Upper Campanian, Cretaceous			
Composition (%)	Quartz	81.3	84.1	67.4	86.5
	Rock fragments	8.1	5.9	5.0	5.3
	Feldspar	0.5	< 0.1	0.4	---
	Mica	0.5	< 0.1	< 0.1	---
	Heavy minerals	< 0.1	< 0.1	0.2	0.6
	Clay minerals	6.9	5.6	22.2	7.3
	Opake matter	2.7	1.5	4.8	0.3
	Calcite	---	2.6	---	---
	Gypsum	---	0.3	---	---
Matrix-grain-relation	Matrix-grain-ratio (-)	0.11	0.11	0.37	0.08
Grain size characteristics	Mean grain size (mm)	0.17	0.16	0.13	0.17
	Sorting	1.49 - moderate	1.39 - good	1.35 - good	1.47 – moderate
Grain contacts	Type of grain contacts	mainly point contacts	mainly point or long contacts	mainly point or long contacts	mainly point contacts
	Number of grain contacts per cm^2 (thin section analysis)	~ 2850	~ 3900	~ 6000	~ 4000
Porosity characteristics	Density (g/cm^3)	2.60	2.68	2.63	2.61
	Bulk density (g/cm^3)	1.87	1.83	1.91	1.76
	Total porosity (Vol.-%)	28.2	31.6	27.2	32.6
	Median pore radius (µm)	~ 110	~ 75	~ 12	~ 95
	Median radius of pore entries (µm)	17.9	15.1	3.2	22.6
	Pore surface (m^2/cm^3)	1.81	0.66	4.81	0.33
Ultrasonic velocity	a – Parallel to bedding (km/s)	2.2	2.6	2.1	1.3
	b – Perpendicular to bedding (km/s)	1.8	2.2	1.6	1.2
	Anisotropy index a/b	1.2	1.2	1.3	1.1
Drilling resistance	Perpendicular to bedding (-)	0.9	1.1	1.2	0.5

Fig. 7. Petrographical properties of Gebel-el-Silsila sandstones.

2.3. Sandstone 3

This yellow-brown sandstone is composed of quartz (main component), clay minerals (kaolinite, clinochlore), rock fragments, opaque matter, feldspar (microcline, albite), heavy minerals and mica (muscovite, biotite). Compared with the other sandstones, it shows the lowest contents of quartz and rock fragments, but the highest contents of clay minerals and opaque matter. Color banding and alignment of mica and longish quartz grains are characteristic. The content of

matrix minerals and the matrix-grain-ratio are high. The sandstone can be classified as lithic graywacke.

The sandstone is very fine- to fine-grained. The proportion of grains in the class of coarse silt is low, high in the class of very fine sand, high (main peak) in the class of fine sand and very low in the classes of medium sand and coarse sand. Compared with the other sandstones, it shows the highest proportion of grains in the class of very fine sand and the lowest proportion of grains in the class of medium sand. The sorting of the sandstone is good and better than the other sandstones. Point contacts and long contacts of the grains are dominant. Compared with the other sandstones, it has a very high number of grain contacts.

The total porosity of the sandstone is high. Interparticle porosity is characteristic. In contrast to the other sandstones, it shows – besides a high proportion of large capillary pores – considerable proportions of smaller capillary pores and micropores. Compared with the other sandstones, it is characterized by the smallest median pore radius and the smallest median radius of pore entries, its ratio between median radius of pore entries and its median pore radius is the highest. It also shows the largest pore surface.

The sandstone is characterized by rather low ultrasonic velocities and low drilling resistance (hardness). The anisotropy index reveals remarkable anisotropical properties of the sandstone.

2.4. Sandstone 4

This white sandstone is composed of quartz (main component), clay minerals (kaolinite, clinochlore), rock fragments, heavy minerals and opaque matter. In contrast to the other sandstones, no feldspar and mica occur in this sandstone. The content of matrix minerals and, thus, the matrix-grain-ratio is low. The sandstone can be classified as sublitharenite to quartzarenite.

The sandstone is fine-grained. The proportion of grains in the class of coarse silt is low, medium in the class of very fine sand, very high (main peak) in the class of fine sand, medium in the class of medium sand and very low in the class of coarse sand. Compared with the other sandstones, it shows the lowest proportion of grains in the class of coarse sand. The sorting of the sandstone is moderate. Point contacts of the grains are dominant. Compared with the other sandstones, it shows – like sandstone 2 - a medium number of grain contacts.

The total porosity of the sandstone is very high. Interparticle porosity is characteristic. Large capillary pores with large pore entries are dominant. The proportion of micropores is very low. Compared with the other sandstones, it shows the largest median radius of pore entries, but the smallest pore surface.

The very low ultrasonic velocities and very low drilling resistance of this sandstone is striking. Anisotropical properties of the sandstone are not very significant.

3. Classification and registration of weathering forms

The characterization, quantification and rating of the weathering state of the stone monuments in Upper Egypt is an important objective of this research project. The systematic investigation of the weathering state must consider different scales of stone deterioration. According to VILES et al. [9] a subdivision into nanoscale (< mm), microscale (mm to cm), mesoscale (cm to m) and macroscale (whole facades or monuments) of stone deterioration can be made. The nanoscale mainly corresponds to non-visible stone deterioration, whereas microscale, mesoscale and macroscale relate to visible stone deterioration.

In the framework of the pilot studies on the sandstone monuments in Upper Egypt, weathering forms on the sandstones were investigated, providing descriptions of stone deterioration phenomena at the mesoscale. Weathering forms represent an important parameter for the characterization and quantification of stone weathering.

A survey of weathering forms on the Gebel el-Silsila sandstones was made at Karnak Temple and Luxor Temple for assessing the range of weathering forms and their intensities. Examples of

different weathering forms are presented in Figures 8 – 13. The survey of weathering forms was the basis for the development of a classification scheme that allows the objective and reproducible registration and quantification of the weathering forms on the sandstones. For this, the standard classification scheme of weathering forms, developed by the Aachen working group "Natural stones and weathering" (FITZNER, HEINRICHS & KOWNATZKI [10], FITZNER & HEINRICHS [11]), was modified and tailored to fit the sandstone monuments in Upper Egypt. The classification scheme comprises four *groups of weathering forms* at the uppermost level I of differentiation:

- group 1 – loss of stone material (LS),
- group 2 – discoloration / deposits (DD),
- group 3 – detachment of stone material (DT),
- group 4 – fissures / deformation (FD).

At level II, each group of weathering forms is subdivided into *main weathering forms*. These are further specified by means of *individual weathering forms* at level III of differentiation. At the most detailed level IV of the classification scheme, each individual weathering form is further differentiated according to intensity. Symbols are proposed for the recording of the weathering forms.

Based on this classification scheme, weathering forms were registered on many pilot areas at Karnak Temple and Luxor Temple considering different ages / construction phases, lithotypes, monument exposure characteristics and previous preservation measures (Fig. 14). Two modes of registration were applied:

- inventory of weathering forms (investigation areas 1 – 18),
- mapping of weathering forms (investigation areas 19 – 21).

The inventory of weathering forms included the listing, description and photodocumentation of weathering forms with estimation of their frequency and with additional information on the range of their intensities. This mode of registration allowed an initial, semi-quantitative synopsis of the spectrum of weathering forms.

The monument mapping method has been developed by the Aachen working group "Natural stones and weathering" as a non-destructive procedure for the very detailed registration, documentation and evaluation of weathering forms (e.g. FITZNER & HEINRICHS [11]). It can be applied to all stone types and to all kinds of stone objects ranging from sculptures to facades or entire monuments. Today, monument mapping still represents the only method, which allows us to describe and evaluate whole stone surfaces precisely and reproducibly according to type, intensity and distribution of weathering forms. Three pilot areas (19, 20, 21) at Karnak Temple were mapped in detail (Fig. 14). These pilot areas are of quite different ages:

- mapping area 19: Third Intermediate Period, 22nd–23rd Dynasty, 944–732 BC,
- mapping area 20: New Kingdom, 20th Dynasty, 1190 – 1075 BC,
- mapping area 21: New Kingdom, 18th Dynasty, 1540 – 1292 BC.

The most differentiated level IV of the classification scheme of weathering forms developed for the sandstone monuments in Upper Egypt was used for mapping. So, all individual weathering forms and their intensities were registered and documented in tailor-made plans of the mapping areas. All weathering forms were illustrated in maps and were evaluated quantitatively. Examples are presented in FITZNER & HEINRICHS [11].

All the main weathering forms observed at Karnak Temple and Luxor Temple, their differentiation into individual weathering forms and the frequency of these individual weathering forms in the investigated areas 1 - 21 are presented in Fig. 15. With respect to the most

characteristic individual weathering forms, their classification of intensities and the range of their intensities at the investigation areas 1 - 21 are shown in Fig. 16.

The results reveal a wide range of weathering forms and intensities and very different spectra and combinations of weathering forms on the different investigation areas composed of Gebel el-Silsila sandstones.

All investigation areas have suffered loss of stone material (*group 1 of weathering forms*). Characteristic *main weathering forms* are back weathering (W) - uniform loss of stone material parallel to the stone surface -, relief (R) - morphological change of the stone surface due to partial or selective weathering - and break out (O) - loss of compact stone fragments. Back weathering due to loss of scales (sW), rounding / notching (Ro), alveolar weathering (Ra), weathering out dependent on stone structure (tR) and break out due to non-recognizable cause (oO) represent the most frequent *individual weathering forms* related to these main weathering forms.

The depths of back weathering due to loss of scales (sW) are mainly in the ranges of 0.5 – 1 cm (intensity 2), 1 – 3 cm (intensity 3) or 3 – 5 cm (intensity 4). The depths of rounding / notching (Ro), alveolar weathering (Ra) and weathering out dependent on stone structure (tR) are mainly in the ranges of < 0.5 cm (intensity 1), 0.5 – 1 cm (intensity 2), 1 – 3 cm (intensity 3) or 3 – 5 cm (intensity 4). Rarely, depths of back weathering due to loss of scales (sW) and rounding / notching (Ro) up to more than 25 cm at maximum were found (intensity 7).

The volume of break out due to non-recognizable cause (oO) mainly amounts to 10 – 125 cm^3 (intensity 2) or 125 – 500 cm^3 (intensity 3).

Besides loss of stone material, all investigated areas show weathering forms involving discoloration / deposits (*group 2 of weathering forms*). Discoloration (D) - alteration of the original stone color -, soiling (I) – dirt deposits on the stone surface -, loose salt deposits (E) - poorly adhesive deposits of salt aggregates - and crust (C) - strongly adhesive deposits on the stone surface - are the characteristic *main weathering forms*. Soiling by particles from the atmosphere (pI), efflorescences (Ee) and light-colored crust changing the morphology of the stone surface (hiC) – here compact, whitish salt crusts - represent the most frequent *individual weathering forms*, which, however, all mainly occur with low intensity (intensity 1).

Additionally, weathering forms characterizing current detachment of stone material were found on all investigation areas (*group 3 of weathering forms*). Characteristic *main weathering forms* are granular disintegration (G) - detachment of individual grains or small grain aggregates -, contour scaling (S) – detachment of larger, platy stone pieces parallel to the stone surface, but not following any stone structure - and granular disintegration to crumbly disintegration (G-P) – transitional form between granular disintegration (G) and crumbly disintegration (P, detachment of larger compact stone pieces of irregular shape). Granular disintegration into sand (Gs), single scale (eS) and granular disintegration into sand to crumbling (Gs-Pu) represent the most frequent *individual weathering forms.* The intensities of granular disintegration into sand (Gs) and granular disintegration into sand to crumbling (Gs-Pu) are mainly low (intensity 1). The thicknesses of the single scales (eS) are mainly in the ranges of 0.5 – 1 cm (intensity 2) and especially 1 – 3 cm (intensity 3). Rarely, single scales with a thickness of more than 5 cm occur.

Furthermore, fissures (L) – individual fissures or systems of fissures due to natural or constructional causes - are characteristic for all investigation areas (*group 4 of weathering forms*). They occur either independently of stone structure (vL) or dependent on stone structure (tL). Very frequently, their intensity is high.

Fig. 8. Weathering form “weathering out dependant on stone structure (tR)”.

Fig. 9. Weathering form “relief due to anthropogenic impact (aR)”.

Fig. 10. Weathering form “break out due to non-recognizable cause (oO)”.

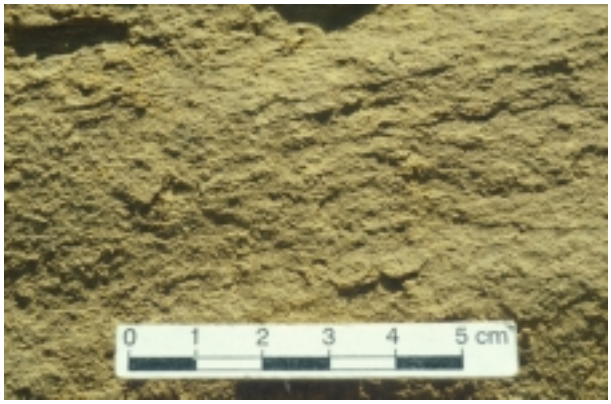

Fig. 11. Weathering form “granular disintegration into sand (Gs)”.

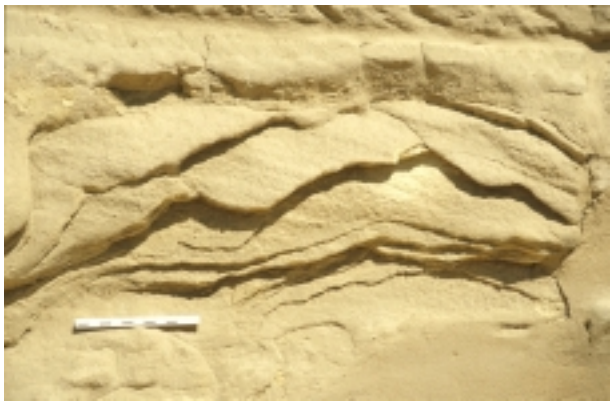

Fig. 12. Weathering form “multiple scales (mS)”.

Fig. 13. Weathering form “fissures independent of stone structure (vL)”.

KARNAK TEMPLE

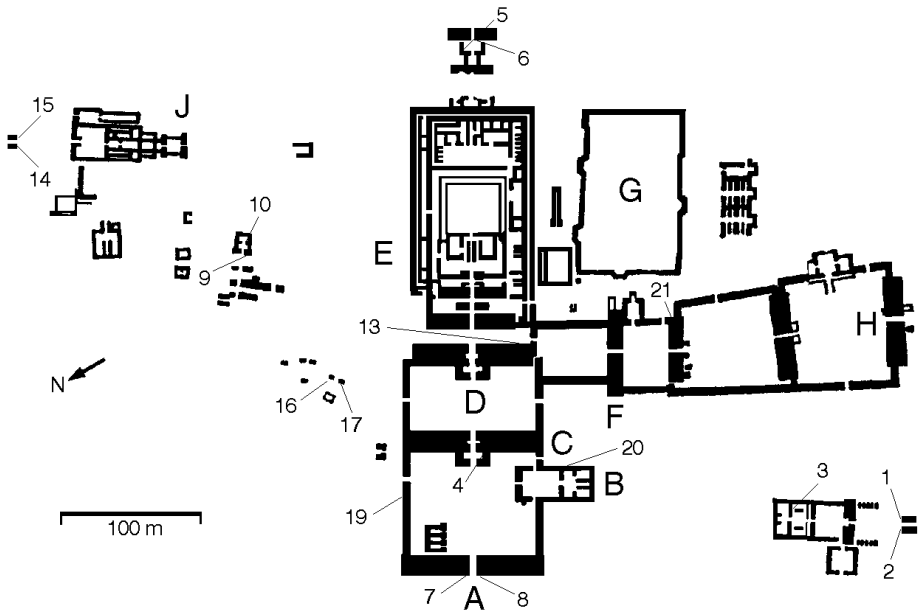

A. First Pylon, main entrance

B. Temple of Ramesses III

C. Second Pylon

D. Great Hypostyle Hall

E. Temple of Amun-Re

F. Seventh Pylon

G. Sacred lake

H. Tenth Pylon

J. Temple of Monthu

Investigation areas

1. Gate of Ptolemy III Euergetes, NNE-facade, part 1
2. Gate of Ptolemy III Euergetes, NNE-facade, part 2
3. Temple of Khonsu, Hypostyle Hall, part - SSW-facade
4. Second Pylon, part - NNE-facade
5. Temple of Ramesses II, part - SSW-facade
6. Temple of Ramesses II, part - WNW-facade
7. First Pylon, WNW-facade, part 1
8. First Pylon, WNW-facade, part 2
9. Temple of Ptah, NW-facade, part 1
10. Temple of Ptah, NW-facade, part 2
13. Third Pylon, part - SE-facade
14. North gate, SSW-facade, part 1
15. North gate, SSW-facade, part 2
16. Chapel of the 26th Dynasty, NW-facade, part 1
17. Chapel of the 26th Dynasty, NW-facade, part 2
19. Great Court, part – NNE-facade, mapping
20. Temple of Ramesses III, part – ESE-facade, mapping
21. Eighth Pylon, ESE-facade, mapping

LUXOR TEMPLE

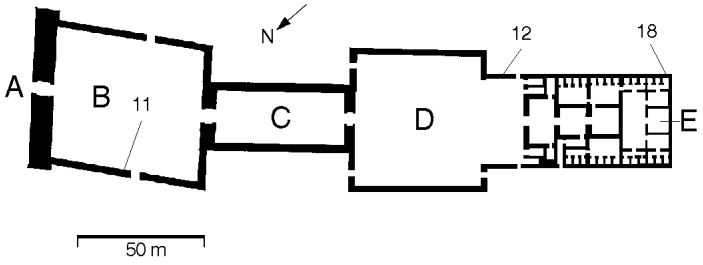

A. First Pylon

B. Court of Ramesses II

C. Colonnade

D. Court of Amenhotep III

E. Naos

Investigation areas

11. Court of Ramesses II, part - SE-facade
12. Hpyostyle Hall, part - ESE-facade
18. Naos, part - ESE-facade

Fig 14. Investigation areas at Karnak Temple and Luxor Temple.

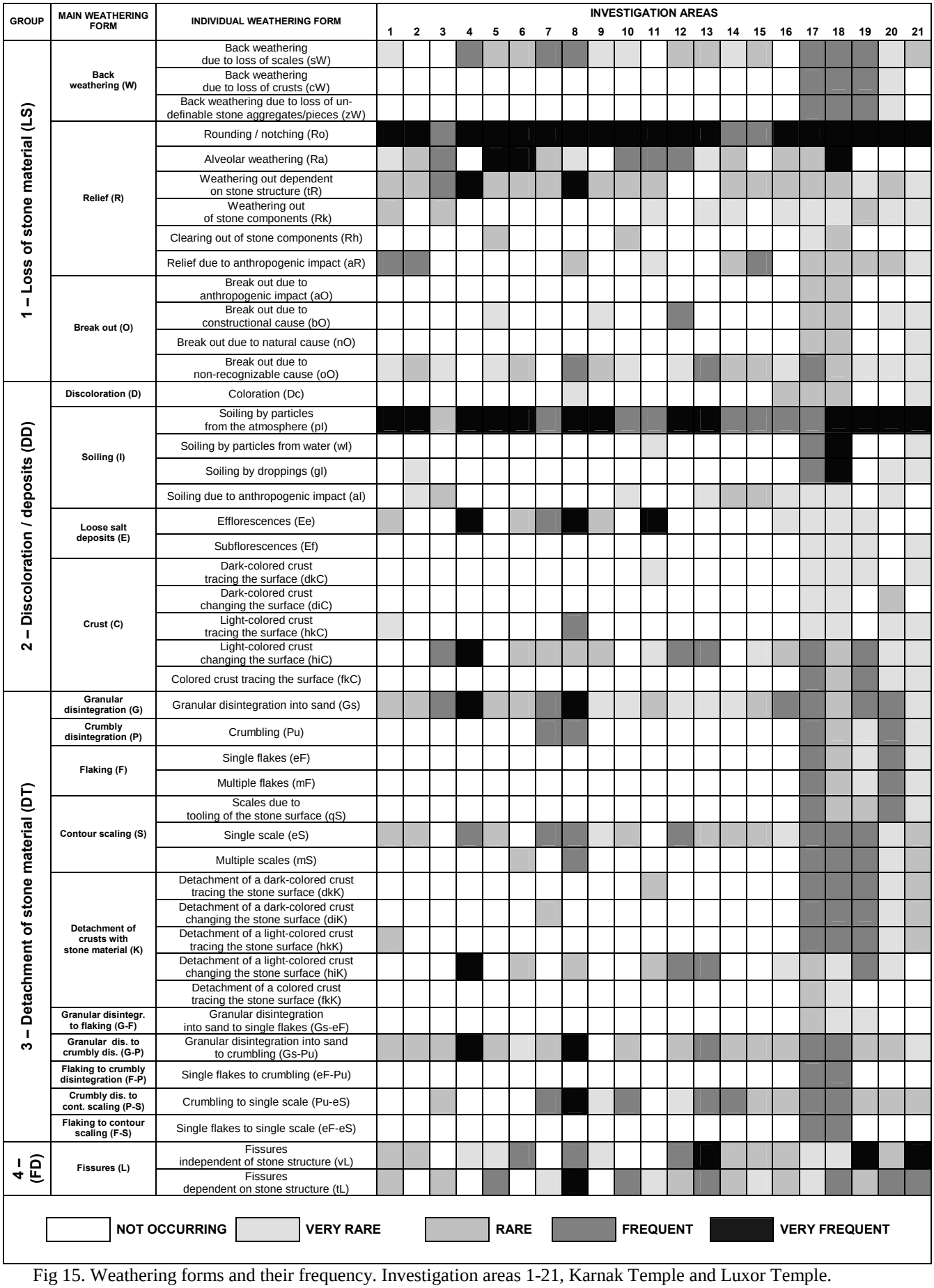

Fig 15. Weathering forms and their frequency. Investigation areas 1-21, Karnak Temple and Luxor Temple.

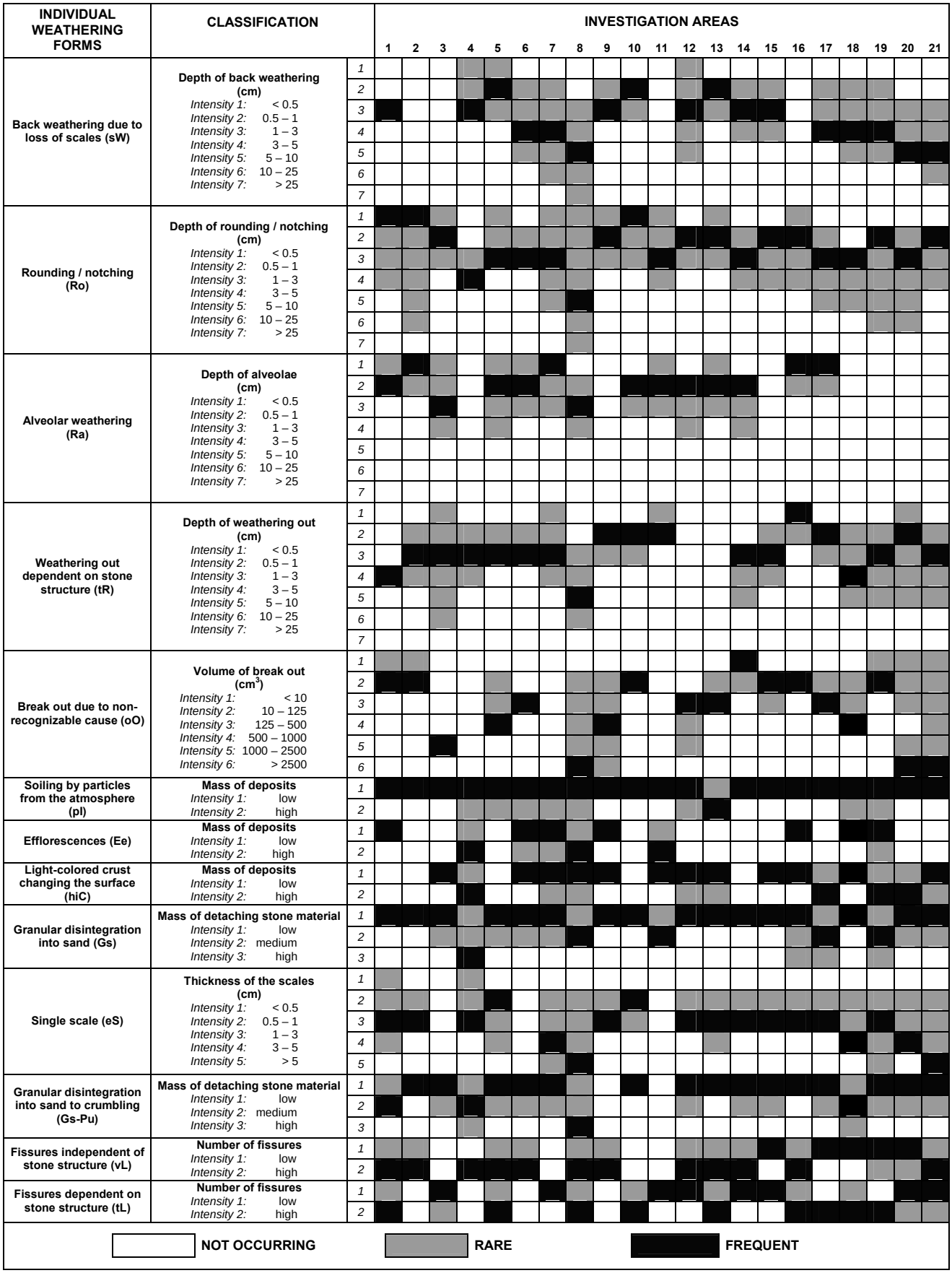

Fig. 16. Intensities of characteristical weathering forms. Investigation areas 1-21, Karnak Temple and Luxor Temple.

4. Quantification and rating of stone damage

Based on the classification and registration of weathering forms and their intensities, damage categories and damage indices were established for quantification and rating of weathering damage (FITZNER & HEINRICHS [11], FITZNER, HEINRICHS & LA BOUCHARDIERE [12]). Six damage categories were defined: 0 – no visible damage, 1 – very slight damage, 2 – slight damage, 3 – moderate damage, 4 – severe damage, 5 – very severe damage. A correlation scheme was developed for the sandstone monuments in Upper Egypt, in which all observed weathering forms – considering their type and intensity - are related to damage categories (Fig. 17). The high historical and artistical value of the Egyptian monuments was taken into account. Based on this correlation scheme, damage categories were determined separately for the four groups of weathering forms (DCLS, DCDD, DCDT, DCFD). In the next step of evaluation, a scheme was elaborated for the derivation of final damage categories (DCAW) jointly considering all groups of weathering forms (Fig. 18). An example for the determination of the final damage category (DCAW) is presented in Fig. 19.

The damage categories were illustrated in maps. The maps of damage categories – considering all groups of weathering forms – are presented for the investigation areas 19 – 21 at Karnak Temple in Fig. 20. The maps outline susceptible parts of monument surfaces and zonation of damage. They enhance risk prognosis and indicate need and urgency of preservation measures. They indicate those parts of monuments on which interventions should focus.

The damage categories were evaluated quantitatively and the damage indices - linear damage index and progressive damage index - were determined (Fig. 21). The linear damage index (DI_{lin}) corresponds to the average damage category, whereas the progressive damage index (DI_{prog}) emphasizes the proportion of higher damage categories (FITZNER, HEINRICHS & LA BOUCHARDIERE [12]).

The three investigation areas 19 – 21 show considerable proportions of moderate, severe or even very severe damage. Considering the possible range of the linear and the progressive damage index between 0 and 5.0 per definition, the damage indices determined for these areas indicate a moderate (investigation areas 20 and 21) to high (investigation area 19) degree of damage. The damage indices do not correlate with the age of the three areas.

Loss of stone material (LS)	**Back weathering (W)**	Back weathering due to loss of scales (sW), back weathering due to loss of crusts (cW), back weathering due to loss of undefinable stone aggregates/pieces (zW)	*Intensities*	*Depth of back weathering (cm)*						
				< 0.5	*0.5 – 1*	*1 - 3*	*3 - 5*	*5 - 10*	*10 - 25*	*> 25*
			Damage cat. (DCLS)	***1***	***1***	***2***	***3***	***4***	***5***	***5***
	Relief (R)	Rounding / notching (Ro), alveolar weathering (Ra), weathering out dependent on stone structure (tR), weathering out of stone components (Rk), clearing out of stone components (Rh), relief due to anthropogenic impact (aR)	*Intensities*	*Depth of relief (cm)*						
				< 0.5	*0.5 – 1*	*1 - 3*	*3 - 5*	*5 - 10*	*10 - 25*	*> 25*
			Damage cat. (DCLS)	***1***	***1***	***2***	***3***	***4***	***5***	***5***
	Break out (O)	Break out due to anthropogenic impact (aO), break out due to constructional cause (bO), break out due to natural cause (nO), break out due to non-recognizable cause (oO)	*Intensities*	*Volume of break out (cm^3)*						
				< 10	10 - 125	125 - 500	500 – 1000	1000 - 2500	> 2500	
			Damage cat. (DCLS)	***1***	***2***	***3***	***3***	***4***	***5***	
Discoloration / deposits (DD)	**Discoloration (D)**	Coloration (Dc)	*Intensities*	*Degree – change of color*						
				low				*high*		
			Damage cat. (DCDD)	***1***				***1***		
	Soiling (I)	Soiling by particles from the atmosphere (pI), soiling by particles from water (wI), soiling by droppings (gI), soiling due to anthropogenic impact (aI)	*Intensities*	*Mass of deposits*						
				low				*high*		
			Damage cat. (DCDD)	***1***				***1***		
	Loose salt deposits (E)	Efflorescences (Ee), Subflorescences (Ef)	*Intensities*	*Mass of deposits*						
				low				*high*		
			Damage cat. (DCDD)	***1***				***2***		
	Crust (C)	Dark-colored crust tracing the surface (dkC), dark-colored crust, changing the surface (diC), light-colored crust tracing	*Intensities*	*Mass of deposits*						
				low				*high*		
			Damage cat. (DCDD)	***2***				***3***		
Detachment of stone material (DT)	**Granular disintegration (G)**	Granular disintegration into sand (Gs)	*Intensities*	*Mass of detaching stone material*						
				low		*medium*			*high*	
			Damage cat. (DCDT)	***1***		***2***			***3***	
	Crumbly disintegration (P)	Crumbling (Pu)	*Intensities*	*Mass of detaching stone material*						
				low		*medium*			*high*	
			Damage cat. (DCDT)	***1***		***2***			***3***	
	Flaking (F)	Single flakes (eF), multiple flakes (mF)	*Intensities*	*Mass of detaching stone material*						
				low		*medium*			*high*	
			Damage cat. (DCDT)	**1**		***2***			***3***	
	Contour scaling (S)	Scales due to tooling of the stone surface (qS), single scale (eS), multiple scales (mS)	*Intensities*	*Thickness of the scales (cm)*						
				< 0.5	*0.5 – 1*	*1 - 3*	*3 - 5*	*> 5*		
			Damage cat. (DCDT)	***1***	***1***	***2***	***3***	***4***		
	Detachment of crusts with stone material (K)	Detachment of a dark-colored crust tracing the stone surface (dkK), detachment of a dark-colored crust changing the stone surface (diK), detachment of a light-colored crust	*Intensities*	*Mass of detaching stone material*						
				low		*medium*			*high*	
			Damage cat. (DCDT)	***1***		***2***			***3***	
	Granular disintegration to flaking (G-F)	Granular disintegration, into sand to single flakes (Gs-eF)	*Intensities*	*Mass of detaching stone material*						
				low		*medium*			*high*	
			Damage cat. (DCDT)	***1***		***2***			***3***	
	Granular to crumbly disintegration (G-P)	Granular disintegration into sand to crumbling (Gs-Pu)	*Intensities*	*Mass of detaching stone material*						
				low		*medium*			*high*	
			Damage cat. (DCDT)	***1***		***2***			***3***	
	Flaking to crumbly disintegration (F-P)	Single flakes to crumbling (eF-Pu)	*Intensities*	*Mass of detaching stone material*						
				low		*medium*			*high*	
			Damage cat. (DCDT)	***1***		***2***			***3***	
	Flaking to crumbly disintegration (F-P)	Single flakes to crumbling (eF-Pu)	*Intensities*	*Mass of detaching stone material*						
				low		*medium*			*high*	
			Damage cat. (DCDT)	***1***		***2***			***3***	
	Crumbly disintegration to contour scaling (P-S)	Crumbling to single scale (Pu-eS)	*Intensities*	*Mass of detaching stone material*						
				low		*medium*			*high*	
			Damage cat. (DCDT)	***1***		***2***			***3***	
	Flaking to contour scaling (F-S)	Single flakes to single scale (eF-eS)	*Intensities*	*Mass of detaching stone material*						
				low		*medium*			*high*	
			Damage cat. (DCDT)	***1***		***2***			***3***	
(FD)	**Fissures (L)**	Fissures independent of stone structure (vL), fissures dependent on stone structure (tL)	*Intensities*	*Number of fissures*						
				low				*high*		
			Damage cat. (DCFD)	***2***				**3**		

Fig. 17. Correlation scheme “weathering forms – damage categories”

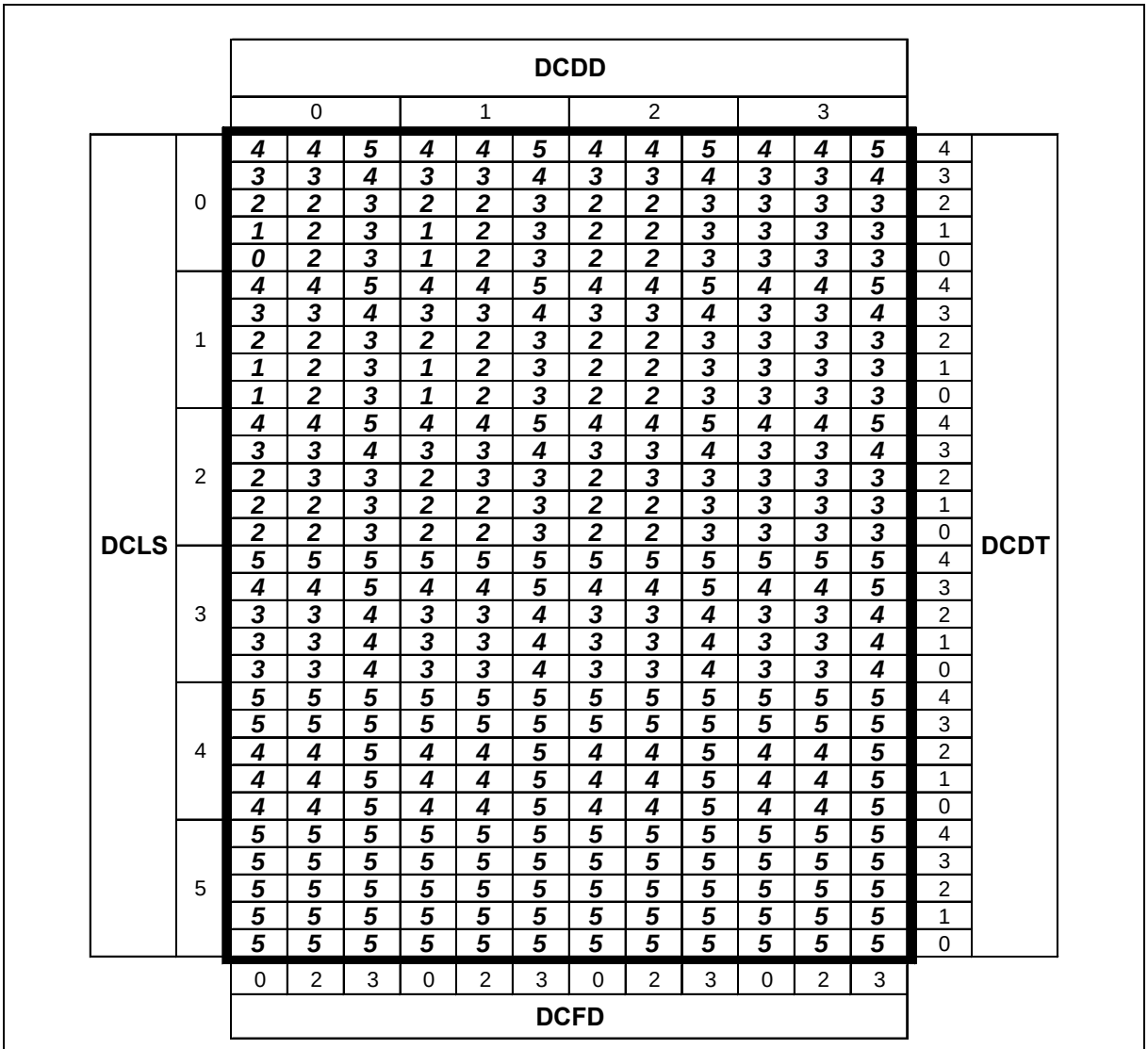

DCLS – Damage categories for all weathering forms of group 1 “loss of stone material“.

DCDD – Damage categories for all weathering forms of group 2 “discoloration/deposits“.

DCDT – Damage categories for all weathering forms of group 3 “detachment“.

DCFD – Damage categories for all weathering forms of group 4 “fissures / deformation“.

DCAW – *Damage categories considering all groups of weathering forms.*

Damage categories					
0	*1*	*2*	*3*	*4*	*5*
no visible damage	***very slight damage***	***slight damage***	***moderate damage***	***severe damage***	***very severe damage***

Fig. 18. Scheme for the determination of damage categories considering all groups of weathering forms.

5. Discussion

In the year 2000 an Egyptian-German research co-operation was started for systematic studies on stone weathering on the historical monuments in Upper Egypt. Sandstones, limestones and granites were used for their construction. In the framework of the initial field work carried out by the German partner, studies were concentrated on Gebel el-Silsila sandstones, which represent the characteristic stone material of the sandstone monuments in Upper Egypt. A survey of the historical quarries was started including sampling. Initial results of the laboratory analyses have shown considerable variation in the sandstones with respect to their petrographical and petrophysical properties. The systematic survey of the quarries, the analyses and classification of the sandstones and their identification on the monuments will be continued. Weathering forms on the Gebel el-Silsila sandstones were studied at Karnak Temple and Luxor Temple. The weathering forms were classified according to type and intensity. Based on this classification scheme – developed for the sandstone monuments in Upper Egypt – the weathering forms and their intensities were registered on many parts of Karnak Temple and Luxor Temple. The results of these first studies have shown a great variety of weathering forms characterizing loss of stone material, discoloration / deposits, current detachment of stone material and fissures / deformation and, additionally, a wide range of their intensities. The results represent an important basis for the statistical evaluation of weathering forms in relation to age and exposure characteristics of the investigation areas, sandstone varieties, environmental conditions and previous preservation measures. Identification of the sandstone varieties used on the monuments as well as the characterization of the environmental conditions will be objectives of planned future works. In addition to description of stone deterioration phenomena by means of weathering forms, damage categories and damage indices were established for the rating of stone damage. A correlation scheme “weathering forms – damage categories” was developed. Damage categories and damage indices were determined for several pilot investigation areas at Karnak Temple, based on detailed mapping of weathering forms. Considerable proportions of severe or even very severe damage were noted for parts of the investigation areas, while other parts have remained in rather good condition. It was found that the degree of damage on the investigated areas – quantified by damage index – does not correlate with their age. The degree of weathering damage appears to be much more dependent on exposure characteristics of the investigation areas and the local environmental conditions, especially as related to salt weathering processes. The considerable frequency of efflorescences and salt crusts – mainly halite and gypsum, rarely sylvite – indicates salt loading of the sandstones as an important weathering factor. This confirms the findings of other authors (e.g. MARTINET [5], BILLARD & BURNS [13], BILLARD, BURNS & WILSON-YANG [14], SALEH et al. [15], BADAWY & ABDEL MONEIM [16], GOUDIE & VILES [17], SMITH [18]). It is an important aim of the Egyptian-German research co-operation to contribute to the explanation of the complex mechanisms of salt weathering on the historical monuments in Upper Egypt which are still not satisfactorily understood.

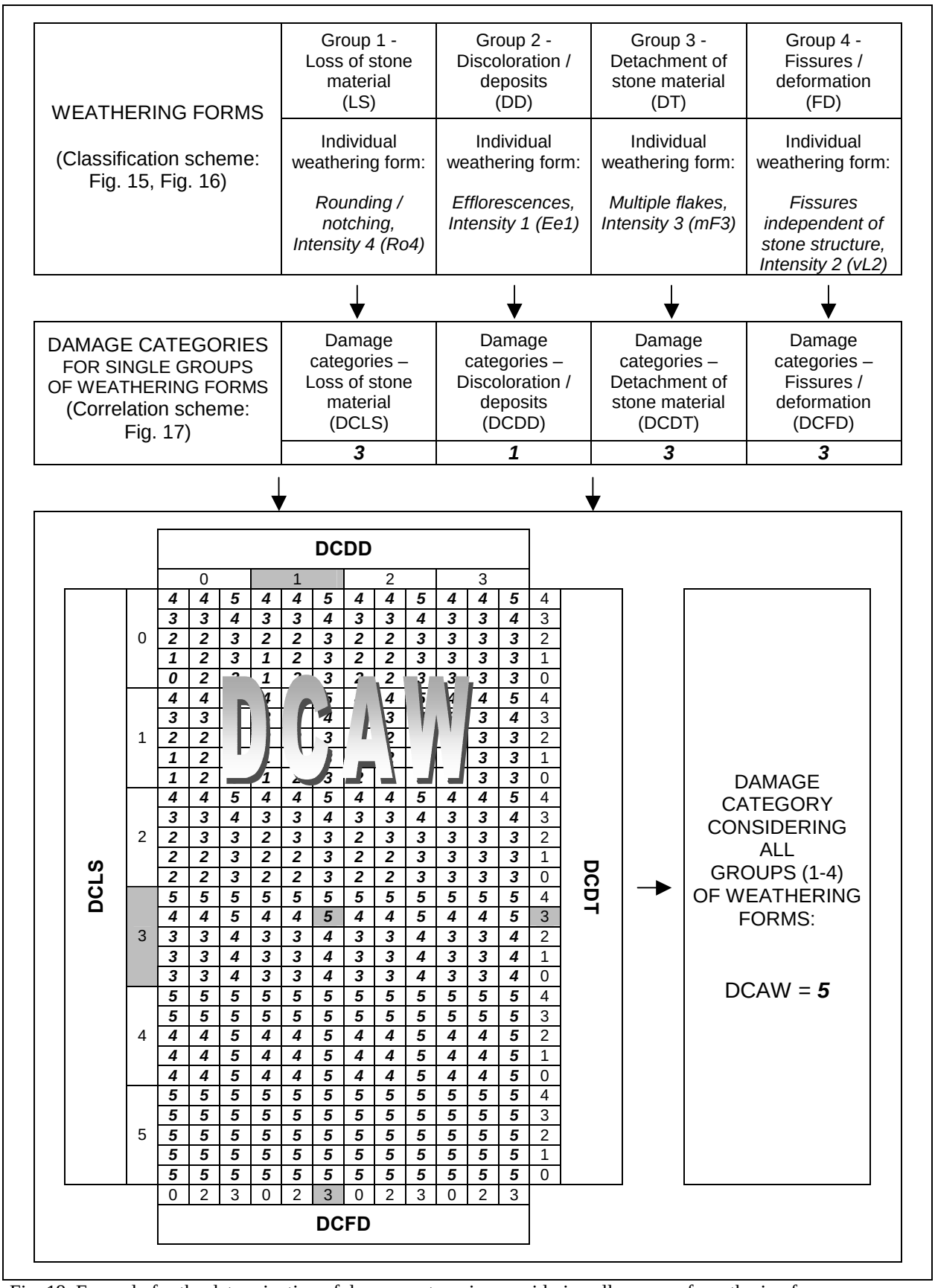

Fig. 19. Example for the determination of damage categories considering all groups of weathering forms.

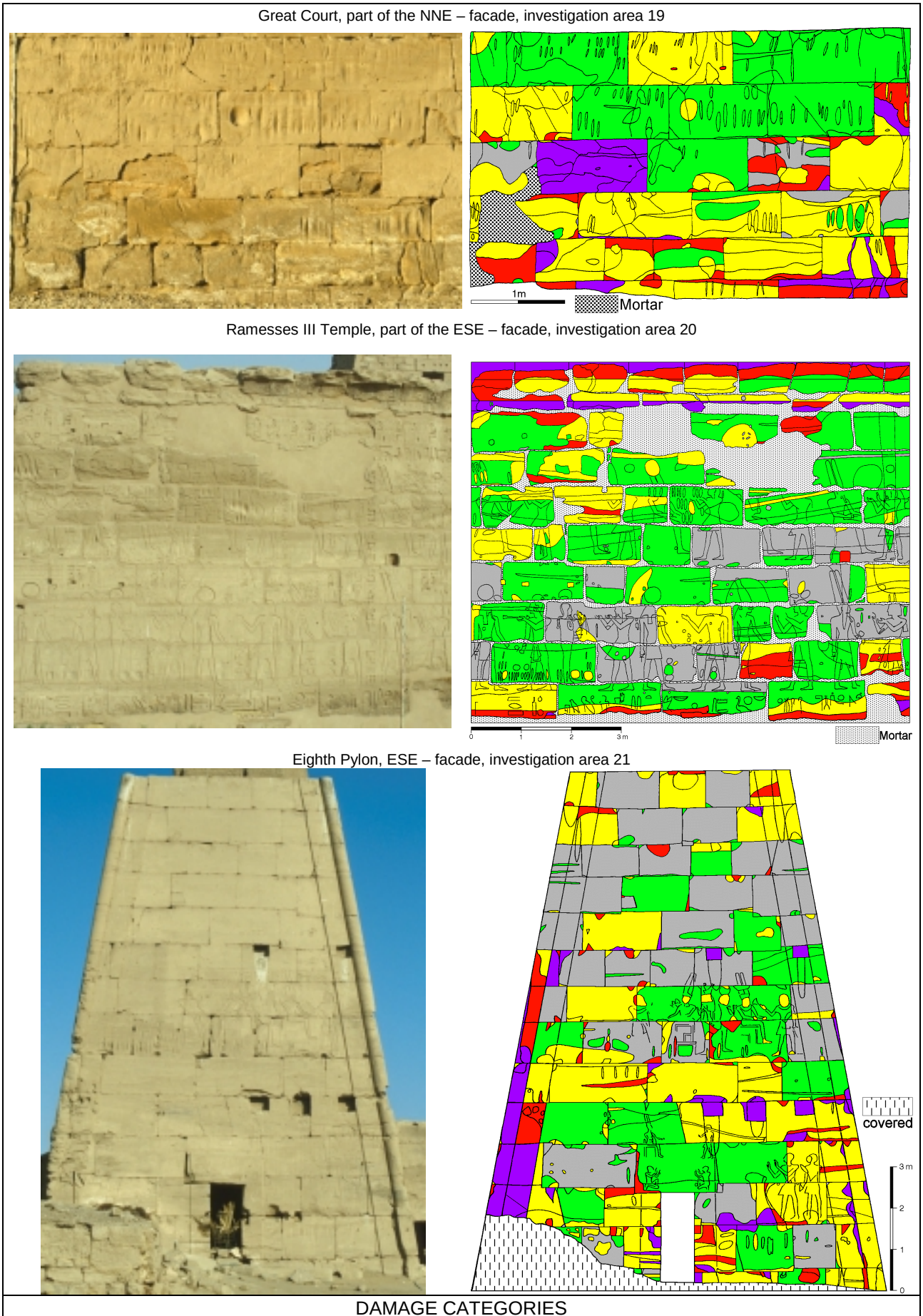

Fig. 20. Damage categories. Investigation areas 19-21, Karnak Temple.

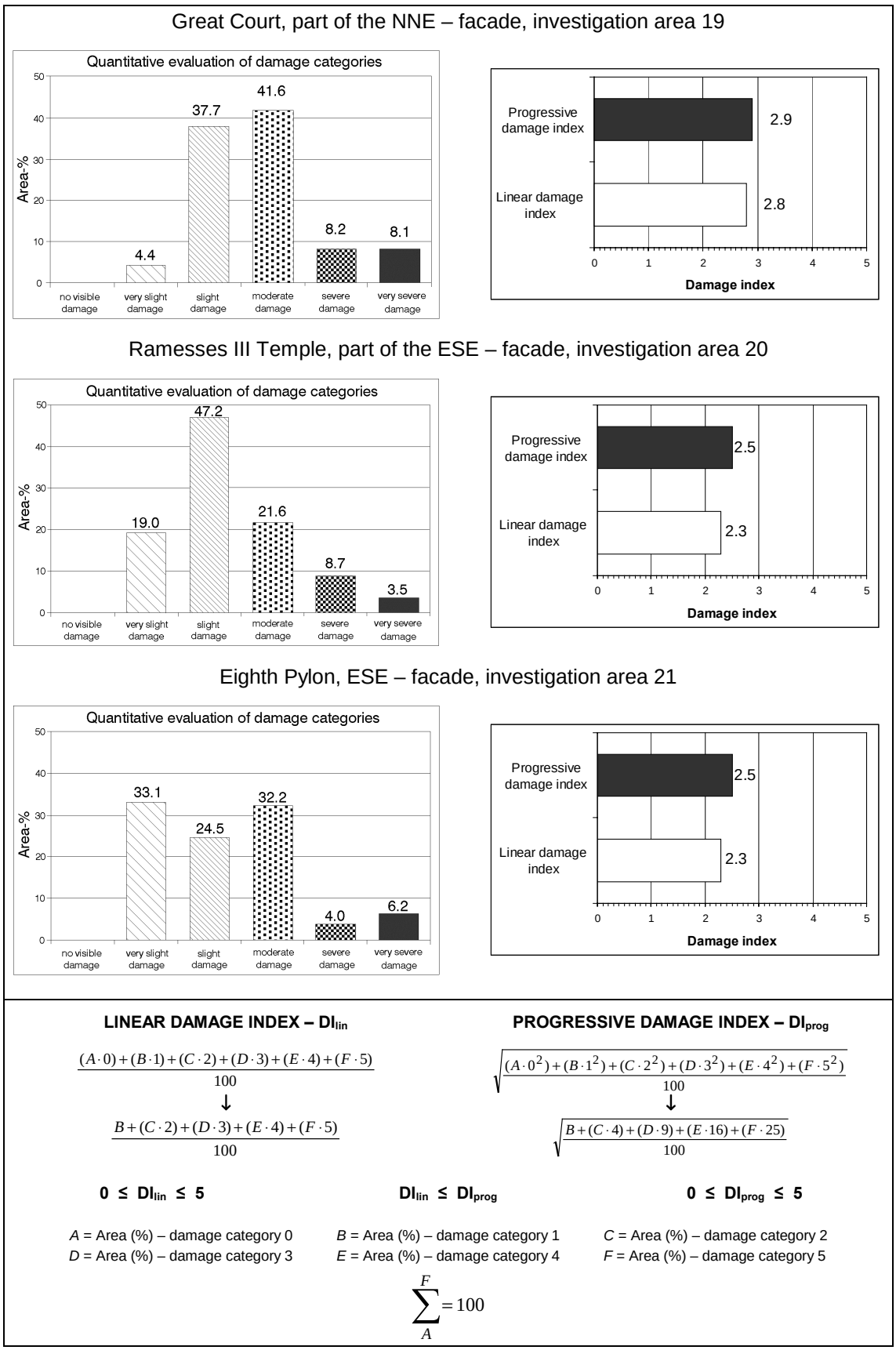

Fig. 21. Quantitative evaluation of damage categories and determination of damage indices. Investigation areas 19-21, Karnak Temple.

6. References

1. Hermina M., Klitzsch, E., List, F.K. (1989): Stratigraphic lexicon and explanatory notes to the Geological map of Egypt 1 : 500.000.- Conoco Inc., Cairo, Egypt.
2. Tawadros E.E. (2001): Geology of Egypt and Libya. A. A. Balkema, Rotterdam, Netherlands.
3. Abd el Hady, M.M. (1988): Durability of monumental sandstone in Upper Egypt. Engineering Geology of Ancient Works, Monuments and Historical Sites. Marinos & Koukis (eds), Balkema, Rotterdam.
4. Abd el Hady, M.M. (2000): The deterioration of Nubian sandstone blocks in the Ptolemaic temples in Upper Egypt. Proceedings of the 9th International Congress on the Deterioration and Conservation of Stone, 19-24 June 2000, Venice – Italy, Volume 2: 783-792, Elsevier, Amsterdam.
5. Martinet G. (1992): Grès et mortiers du temple d' Amon à Karnak (Haute Egypte). Etude des altérations, aide à la restauration. Laboratoire Central des Ponts et Chaussées, Paris.
6. Klemm R., Klemm D. (1993): Steine und Steinbrüche im Alten Ägypten.- Springer Verlag, Berlin - Heidelberg.
7. Pettijohn F.J., Potter, P.E., Siever, R. (1987): Sand and sandstone. Second Edition, Springer-Verlag, New York.
8. Tucker, M.E. (1988): Techniques in Sedimentology.- Blackwell Scientific Publications, Oxford.
9. Viles H.A., Camuffo D., Fitz S., Fitzner B., Lindqvist O., Livingston R.A., Maravellaki P.V., Sabbioni C., Warscheid T. (1997): Group report: What is the state of our knowledge of the mechanisms of deterioration and how good are our estimations of rates of deterioration? In Baer, N. S. & Snethlage, R. (ed.): Report of the Dahlem Workshop on "Saving our architectural heritage: The conservation of historic stone structures", Berlin, March 3-8, 1996: 95-112, John Wiley & Sons Ltd.
10. Fitzner B., Heinrichs K., Kownatzki, R. (1995): Weathering forms – classification and mapping / Verwitterungsformen – Klassifizierung und Kartierung. Denkmalpflege und Naturwissenschaft, Natursteinkonservierung I: 41-88, Verlag Ernst & Sohn, Berlin.
11. Fitzner B., Heinrichs K. (2002): Damage diagnosis on stone monuments – weathering forms, damage categories and damage indices. In Prikryl, R. & Viles, H.A. (ed.): Understanding and managing stone decay, Proceeding of the International Conference "Stone weathering and atmospheric pollution network (SWAPNET 2001)", 11-56, The Karolinum Press, Charles University, Prague, Czech Republic.
12. Fitzner B., Heinrichs K., La Bouchardiere D. (2002): Damage index for stone monuments. In Galan, E. & Zezza, F. (ed.): Protection and Conservation of the Cultural Heritage of the Mediterranean Cities, Proceedings of the 5th International Symposium on the Conservation of Monuments in the Mediterranean Basin, Sevilla, Spain, 5-8 April 2000: 315-326, Swets & Zeitlinger, Lisse, The Netherlands.
13. Billard, T.C., Burns, G. (1980): Mechanisms of Salinization of Great Temples in Luxor Area. Jour. Soc. f. t. Study of Egyptian Antiquities, 10: 243-249, Toronto.
14. Billard, T.C., Burns, G., Wilson-Yang, K.M. (1982): Salinization in the Nile Valley: The Karnak Area. Jour. Am. Res. Center in Egypt, 19: 111-113, Princeton.

15. Saleh S.A., Helmi F.M., Kamal M.M., El-Banna A.-F.E. (1992): Study and consolidation of sandstone: Temple of Karnak, Luxor, Egypt. Studies in Conservation, 37 (2):93-104, London.
16. Badawy I., A. Abdel Moneim A. (1999): Environmental deterioration of Karnak Temples, Luxor, Upper Egypt. Bulletin of the Faculty of Engineering, Assiut University, Vol. 27, No. 1, Egypt.
17. Goudie, A. & Viles, H.A. (1997): Salt weathering hazards. John Wiley & Sons, Ltd., West Sussex, England.
18. Smith, S.E. (1986): An assessment of structural deterioration on ancient Egyptian monuments and tombs in Thebes. Journal of Field Archaeology, 13, 503-510.